Damage detection in slab structures based on two-dimensional curvature mode shape method and Faster R-CNN

Duong Huong Nguyen[1] and Magd Abdel Wahab[2]

[1]*Department of Bridge and Tunnel Engineering, Faculty of Bridges and Roads, Hanoi University of Civil Engineering, Hanoi, Vietnam*
duongnh2@huce.edu.vn
[2]*Soete Laboratory, Faculty of Engineering and Architecture, Ghent University, Technologiepark Zwijnaarde 903, B-9052 Zwijnaarde, Belgium*

∗Corresponding author, Professor M Abdel Wahab: magd.abdelwahab@UGent.be

Abstract

This paper proposes a novel method based on the two-dimensional (2D) curvature mode shape method, Convolutional Neural Networks (CNN), and Faster Region-based Convolutional Neural Networks (faster R-CNN) for detecting damage in slab structures. The 2D curvature mode shape could be measured directly or calculated from the measured mode shape using the central difference method. The damage indicator is defined as the absolute differences between the 2D curvature mode shape of the damaged and intact slabs. The contour plot is chosen to convert the damage indicators into images. Four hundred damage scenarios are created using a Finite Element (FE) model of the slab. Images created from those damage scenarios are then used to train CNN and faster R-CNN. Four damage types are considered in this research. A single small hole, a single big hole, two small holes, and two big holes are considered as damage types. After training, CNN can predict the damage types and faster R-CNN can predict the bounding boxes around the damaged areas. A test sample set is created to test the performance of the proposed method. The effect of noise in the mode shape data is considered. Results show that the classification accuracy for damage type is high. The overlap ratios between the predicted bounding boxes and the real damaged areas are more than 40% for 80% of tested scenarios. Furthermore, the low influence of noise on the predicted results is investigated. The proposed method is robust and has great potential for application to real structures.

Keywords: Damage detection, slab structures**,** convolution neural network (CNN), Faster Region-based Convolutional Neural Networks (faster R-CNN), structural health monitoring (SHM).

1 Introduction

Vibration-based Structural Health Monitoring (SHM) has emerged as one of the most popular methods in the past decades [1-4]. Early detection of the presence of damage may prevent the structure from complete failure. The maintenance work could be done to enhance the bridge's lifetime. The money to build the new bridge or to seriously repair the old bridge could be saved. For this reason, damage detection is one of the most important in the SHM process.

In recent years, many Vibration-Based Damage Detection methods (VBDD) were introduced. The principle of these methods is that modal parameters, such as natural frequency, modal damping, and mode shapes are strongly connected to structural behavior. Mode shapes and curvature mode shapes are worthy parameters that can be directly or indirectly used to detect single or multiple local damages. Pandey et al. [5] presented absolute changes in the curvature mode shapes that could be used to localize

the region of damage in the numerical cantilever and simply supported beam. This approach was then verified, applied, and presented in many papers. For instance, Ratcliffe [6] improved this technique with the gapped smoothing technique and then applied it to detect damage in a beam. Wahab et al. [7] applied this method to Z24 bridge damage detection. The concept of curvature mode shapes was then developed for 2D structure by Wu et al. [8]. The techniques using 2D curvature mode shapes were proposed for detecting damage in composite laminated plates [9]. Several damage indicators were suggested for damage identification in 2D structures. For example, the Mode Shape Data Derivative Based Damage Identification (MSDBDI) index was suggested by Navabian et al. [10], and the damage index using two-dimensional mode shape curvature was evaluated by Zhong et al. [11].

Nowadays, methods that apply machine learning techniques for SHM are highly popular [12, 13]. Neural networks can be used to solve both the forward and inverse problems [14-16] . For SHM issues, a neural network can predict the damage severity and location based on the given input data sets. CNN, which utilizes images as input data, is one of the most popular neural networks. CNN could identify the existence of damage and damage type simply from images [17]. The combination of VBDD with the CNN model was investigated in many works [18-23]. CNN-based SHM method was introduced and verified the sensitiveness with small changes in structural condition [23]. The curvature gapped smoothing method emerged with CNN was proposed to identify damage in beam structures [24], and then was improved for girder bridges [25]. Some researchers tried to apply CNN to detect damage in the 2D structure. Wavelet-based CNN method is used to find damage on rectangular laminated composite plates [26]. The proposed WT-CNN method can predict the existence of damage and its locations. Large-scale experiments were set up to verify the computational efficiency of the proposed method that combines CNN and the real-time damage detection method [18]. This method performs VBDD and localization of the damage in real time.

Faster R-CNN is developed by a group of researchers at Microsoft Research [27]. Faster R-CNN is a deep CNN used for object detection. The network can predict the locations of different objects in a single image accurately and quickly. Faster R-CNN is used to detect and classify damaged roads [28]. The original architecture of Faster R-CNN is proposed to detect and localize multiple types of damage in civil structures [29]. Up to now, most of the applications of CNN and faster R-CNN for SHM are the classification of the images of crack, steel, bolt corrosion, and concrete spalling [13, 30, 31]. The amount of research that uses the combination of VBDD with faster R-CNN is limited.

In the literature, a review on modal parameter-based damage detection methods for beam or 2D structures is introduced in Ref [4]. It was observed that curvature mode shape-based methods focus on damage localization and optimization algorithms need to be applied to precisely locate the damage. Many researchers attempt to follow this direction. Khatir et al. [32] combined Artificial Neural Network (ANN) and an arithmetic optimization algorithm for damage quantification and its position in FGM composite plates. In this research, a damage indicator based on the frequency response functions was employed on the input layer of ANN. In another research, optimization algorithms that use the objective function to minimize the differences of the measured and analyzed displacements and strains could identify the crack in plate structures [33]. Ho et al. [34] proposed an efficient stochastic-based coupled model for damage identification on plate structures. This study indicates that using only the mode shape derivative-based damage identification (MSDBDI) index is very hard to find out the damage severity. However, combining it with the ANN and an optimizer coupled model could overcome this drawback.

To conclude, combining VBDD with an optimization, machine learning algorithm to solve the SHM problem is quite a promising approach. In this paper, a novel method which associates the 2D curvature mode shape method with CNN, and faster R-CNN will be proposed. The 2D curvature can be measured or calculated directly from the displacement mode shape [35, 36]. This method can precisely locate damage and define the severity of damage in slab structures. This paper is organized into five sections. The first section is the introduction part, followed by the second section about the theoretical background of the 2D curvature mode shape method, CNN, and Faster R-CNN. A laboratory steel slab experiment is introduced in Section 3. The damage detection method and results are presented in Section 4. Section 5 is the conclusion section.

2 Theoretical background

2.1 Two-dimensional curvature mode shape of slab structure

Mode shape is one of the dynamic parameters, which is sensitive to damage. Modal curvature based on mode shape derivative is widely used as the damage detection method. Any local damage can change the curvature of mode shapes. For 2D structures, the curvature has three components, longitudinal (ϕ''_{xx}), transversal (ϕ''_{yy}), and torsional (ϕ''_{xy}). Besides direct modal strain measurement, the central finite difference method can be employed to calculate the curvature mode shape.

Equations for longitudinal and transversal components of a 2D curvature mode shape applying the central finite difference method are as follows:

$$\phi''_{xx(x_i,y_j)} = \frac{\phi_{(x_{i+1},y_j)} - 2\phi_{(x_i,y_j)} + \phi_{(x_{i-1},y_j)}}{l_x^2} \tag{1}$$

$$\phi''_{yy(x_i,y_j)} = \frac{\phi_{(x_i,y_{j+1})} - 2\phi_{(x_i,y_j)} + \phi_{(x_i,y_{j-1})}}{l_y^2} \tag{2}$$

Where $\phi_{(x_i,y_j)}$ is the amplitude of displacement mode shape at node (x_i, y_j),

l_x and l_y are the uniform spacing along the *x* and *y* direction.

To determine the torsional component $\phi''_{xy(x_i,y_j)}$, two steps are suggested in Ref [11]. Firstly, equations (3) to (6) are used to calculate T_k of all grid spaces that have node (x_i, y_j) in the corner. Then, the value of torsional curvature at this grid point is found by taking the average of all T_k. If the node (x_i, y_j) is at boundary, two of four T_k components will be equal to zero.

$$T_1 = \frac{\frac{\phi_{(x_{i+1},y_{j+1})} - \phi_{(x_{i+1},y_j)}}{l_y} - \frac{\phi_{(x_i,y_{j+1})} - \phi_{(x_i,y_j)}}{l_y}}{l_x} \tag{3}$$

$$T_2 = \frac{\frac{\phi_{(x_i,y_{j+1})} - \phi_{(x_i,y_j)}}{l_y} - \frac{\phi_{(x_{i-1},y_{j+1})} - \phi_{(x_{i-1},y_j)}}{l_y}}{l_x} \tag{4}$$

$$T_3 = \frac{\frac{\phi_{(x_{i+1},y_j)} - \phi_{(x_{i+1},y_{j-1})}}{l_y} - \frac{\phi_{(x_i,y_j)} - \phi_{(x_i,y_{j-1})}}{l_y}}{l_x} \tag{5}$$

$$T_4 = \frac{\frac{\phi_{(x_i,y_j)} - \phi_{(x_i,y_{j-1})}}{l_y} - \frac{\phi_{(x_{i-1},y_j)} - \phi_{(x_{i-1},y_{j-1})}}{l_y}}{l_x} \quad (6)$$

$$\phi''_{xy(x_i,y_j)} = \frac{T_1 + T_2 + T_3 + T_4}{4} \quad (7)$$

The curvature mode shape at node (x_i, y_j) is calculated as below:

$$\phi''_{(x_i,y_j)} = \sqrt{{\phi''_{xx(x_i,y_j)}}^2 + {\phi''_{xy(x_i,y_j)}}^2 + {\phi''_{yy(x_i,y_j)}}^2} \quad (8)$$

The damage index of the slab structure for the m^{th} mode is described as the difference between the curvatures of the intact and damaged slab at all nodes.

$$DI_m = {\phi''}_{h,m} - {\phi''}_{d,m} \quad (9)$$

Where ${\phi''}_{h,m}$ and ${\phi''}_{d,m}$ are healthy and damaged curvature mode shape.

If multiple modes are considered, the average damage index in all modes is defined as the total damage indexes:

$$DI = \frac{1}{N}\sum_{m=1}^{N} DI_m \quad (10)$$

Where: N is the total number of considered modes.

2.2 Convolutional Neural Network (CNN)

CNN is known as an image classification neural network. CNN predicts an input image belongs to one specified damaged location, which was defined before. The backpropagation algorithm is employed to train the weights matrix W. Filter or kernel can be used to indicate the weight matrix. The output matrix of the convolutional layer l is computed as follows:

$$y^l_{i,j} = g\left(\sum_{a=0}^{n-1}\sum_{b=0}^{n-1} w_{a,b}\, y^{l-1}_{(i+a),(j+b)} + b_{a,b}\right) \quad (11)$$

Where y^{l-1} is the input matrix computed at the previous layer convolved with a kernel matrix g is an activation function, b is the bias matrix, $w_{a,b}$ is the weight matrix, n is the filter matrix size.

There are five types of layers in a typical CNN:

- The input layer receives the input images. Each image is labelled. For example, in this research, images are labelled with damage types.
- Convolutional layer is where filters are put in the input image or other feature maps from the previous convolutional layer. In this layer, the activation function is employed for every value of the feature map. The main feature of images is extracted in this layer.
- The pooling layer is similar to the Convolutional layer. It could be the maximum or average pooling, i.e., it takes the maximum or average value in a certain filter region. This layer helps to reduce the number of neurons in the next layer.
- A fully connected layer is placed before the classification output of a CNN. In this layer, information from the final feature map is aggregated and final classification is generated.
- The output layer is the last layer of neurons that provides the final result of the network (i.e., class or label).

To evaluate the accuracy of a network, the loss function is used to find out the differences between the output results and the labelled values in the training data set. For instance, hinge loss, binary cross-entropy, and cross-entropy are loss functions used for learning classification models.

2.3 Faster R-CNN

Detecting the damage in a 2D structure includes two steps. First, identify the bounding box (rectangular) around the damage location. Second, decide what the object in the boundary box belongs to what type of damage with a percentage of accuracy (confidence score).

Because CNN cannot solve the object detection problem, R-CNNs are proposed [37]. The ideal of R-CNN is simple. First, the Selective Search algorithm is used to estimate approximately 2000 bounding boxes in the input image that have the potential to cover the object. With each bounding box, a class of objects will be predicted. Now, the region proposal needs to be classified. Because the Selective Search algorithm introduces 2000 region proposals, most of these cover no object. Therefore, one class that corresponds to the background is added. Figure 1 shows R-CNN steps to identify the object in a single image.

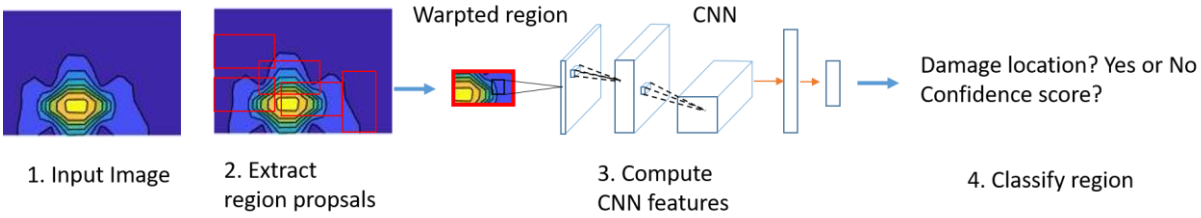

Figure 1. R-CNN steps

However, the Selective Search algorithm is slower when compared to efficient detection networks. 2000 region proposal needs to be classified then the training time is very slow. Fast R-CNN is introduced one year later [38]. Fast R-CNN uses image classification for each image. However, the time to calculate region proposal is still long and the Selective Search algorithm still increases the training and testing time. Therefore, Faster R-CNN was born, and deep learning was used to create region proposals instead of Selective Search algorithm [27]. Faster R-CNN has two modules. The region proposal is proposed in a deep fully convolutional network, which is the first module. Fast R-CNN detector is the second module that uses the proposed regions. A Region Proposal Network (RPN), which is only included in the convolutional layer will estimate an RoI (Region of Interest) region. The input of RPN is the feature map, the output is binary object accuracy score and bounding box regression (to estimate the region, which has an object inside). Based on the object accuracy score, RPN will take 2000, 1000 or even only 100 anchors as the region proposal. RPN helps the fast R-CNN module look for the object region faster. To summarize, all images are passed through the pre-train model to take the feature map first. Then the feature map is used by RPN to propose the region proposals. After that, a fast R-CNN module is applied. The new architecture of faster R-CNN is shown in Figure 2.

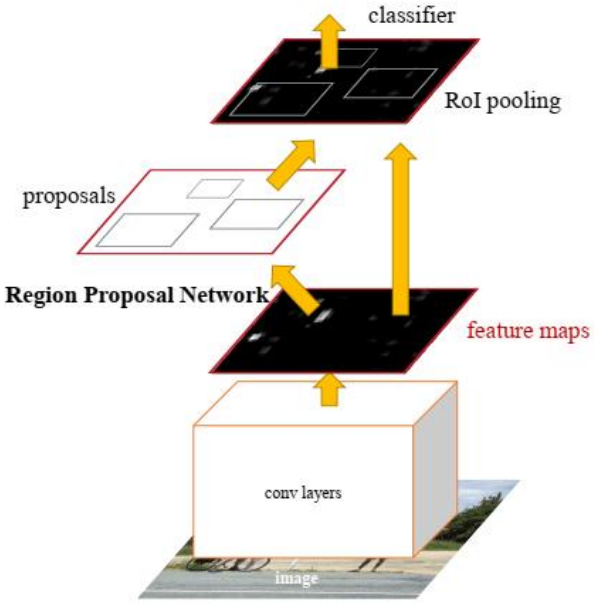

Figure 2. Faster R-CNN architecture [27]

In faster R-CNN, the multi-task loss function has four parts: RPN classification (binary classification, object, or background), RPN regression, Fast-RCNN classification, and Fast-RCNN bounding box regression. Intersection over Union (IoU) is applied in the object detection problem to evaluate the similarity between the predicted bounding box and the real damage location bounding box. The value of IoU is between 0 and 1. IoU is equal to 1 when the real and predicted box is the same. IoU is known as the proportion between the Area of Overlap and the Area of Union. The definition of IoU is illustrated in Figure 3.

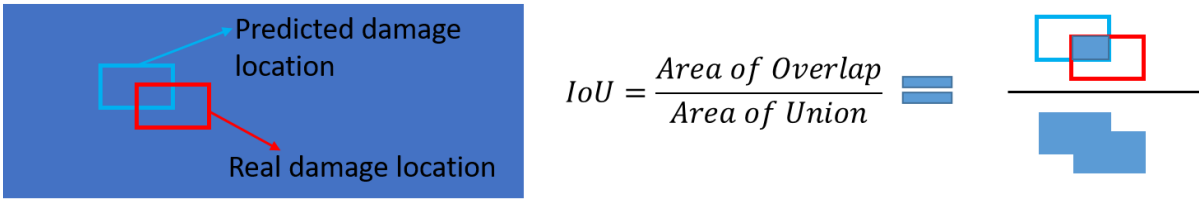

Figure 3. IoU example

Precision measures the accuracy of the model predictions. i.e., the percentage of correct predictions. Precision is defined as a proportion of true positive instances to all positive instances of objects in the detector. Recall measures how good you find all the positives. A ratio of true positive instances to the sum of true positives and false negatives in the detector is defined as the Recall parameter. The average precision (AP) is a way to summarize the precision-recall curve into a single value representing the average of all precisions. The mathematical equation of precision, recall and AP are expressed below:

$$Precision = \frac{TP}{TP + FP} \tag{12}$$

$$Recall = \frac{TP}{TP + FN} \tag{13}$$

$$AP = \sum_{k=0}^{k=n-1} [Recall(k) - Recall(k+1) * Precision(k)] \quad (14)$$

n: number of thresholds

Where TP is True Positive, FP is False Positive and $FN$is False Negative.

3 Model validation

3.1 Experimental setup

Figure 4 shows the experimental setup for a laboratory simply supported steel slab. The length, width, and depth of the slab are 2.5 m, 0.35 m, and 0.01 m, respectively. The effective length or the distance between two supports is 2 m. Figure 4.b and Figure 4.c illustrates the roller support and pinned support, respectively. A notch was cut along the bottom plate of pinned support to eliminate the movement of the roller. For modal measurements, accelerometers were attached to the top of the slab. Four setups were used to measure 44 nodes on the plate. Six nodes were used as the reference nodes. The sensor number and location in each setup are presented in Figure 5.

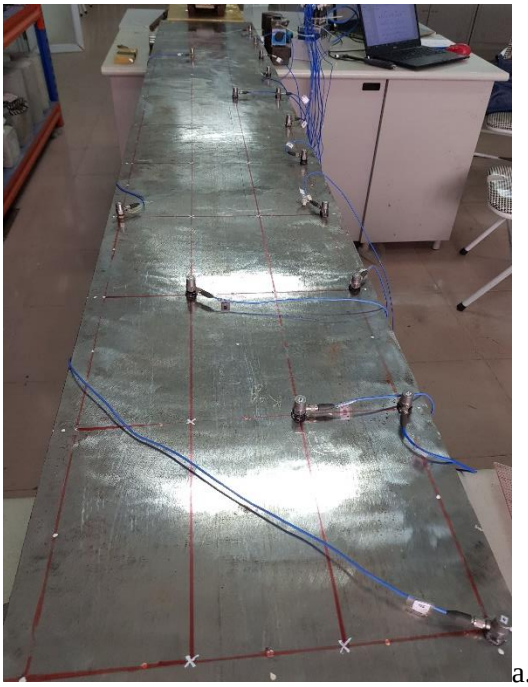
a.

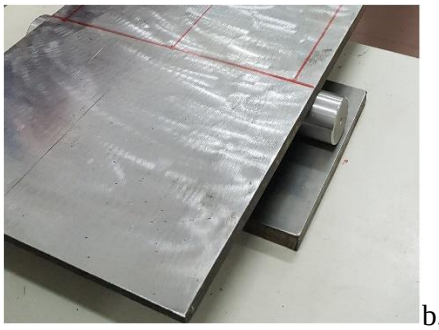
b.

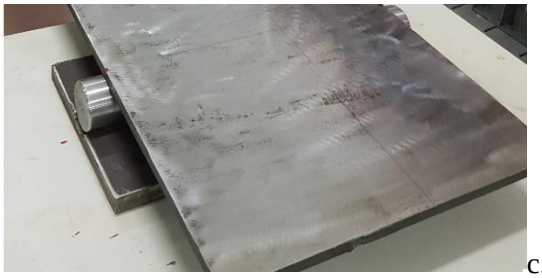
c.

Figure 4. Experimental setup: (a) The steel plate model, (b) roller support and (c) pinned support

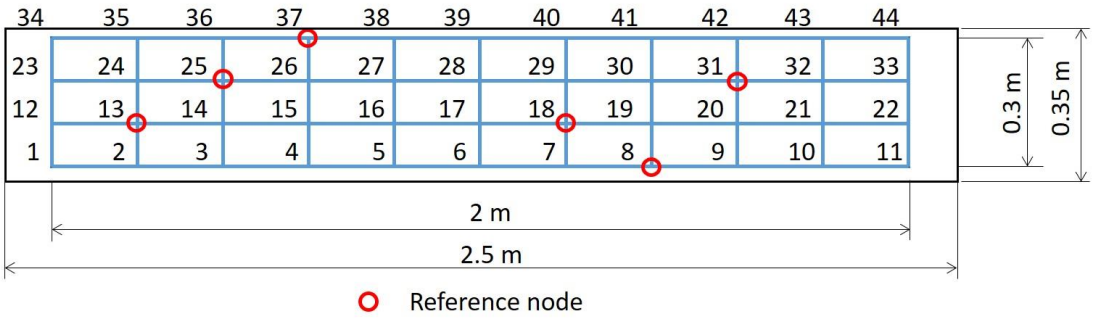

Setup 1: 1, 2, 3, 4, 5, 6, 7, 8, 9, 10, 11, 13, 18, 25, 31, 37
Setup 2: 8, 12, 13, 14, 15, 16, 17, 18, 19, 20, 21, 22, 25, 31, 37
Setup 3: 8, 13, 18, 23, 24, 25, 26, 27, 28, 29, 30, 31, 32, 33, 37
Setup 4: 8, 13, 18, 25, 31, 34, 35, 36, 37, 38, 39, 40, 41, 42, 43, 44

Figure 5. The accelerometer locations and setup

A hammer was used to excite the slab. Each accelerometer weighs approximately 7.8g and has sensitivity from $10.13 - 10.50 \mathrm{mV/m/s^2}$. The sampling frequency and time were 2560Hz and 300 seconds, respectively. The reference-based SSI method [39] was used to analyze vibration data. Figure 6 is the stabilization diagram created by using a stabilization criterion of 1% error in frequency, 5% error in damping, and 98% confidence in mode shape vectors. The stabilization diagram shows four alignments that are present at a minimum model order of 100. The first four bending mode shapes identified from experimental tests are plotted in Figure 7. Although 44 nodes were measured, the experimental mode shapes were expanded to all DOFs in the FE model. A 2D interpolation with grid data set was created.

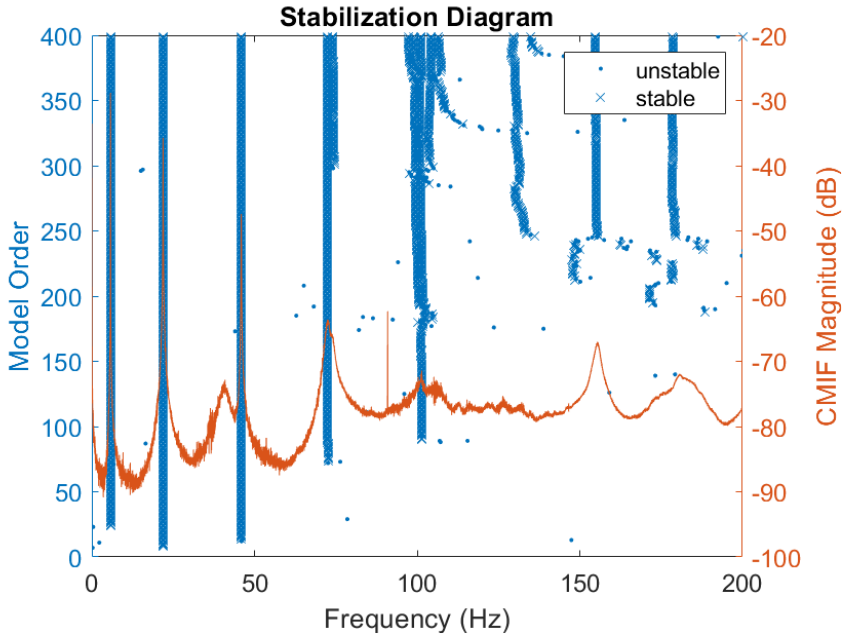

Figure 6. Stabilization Diagram

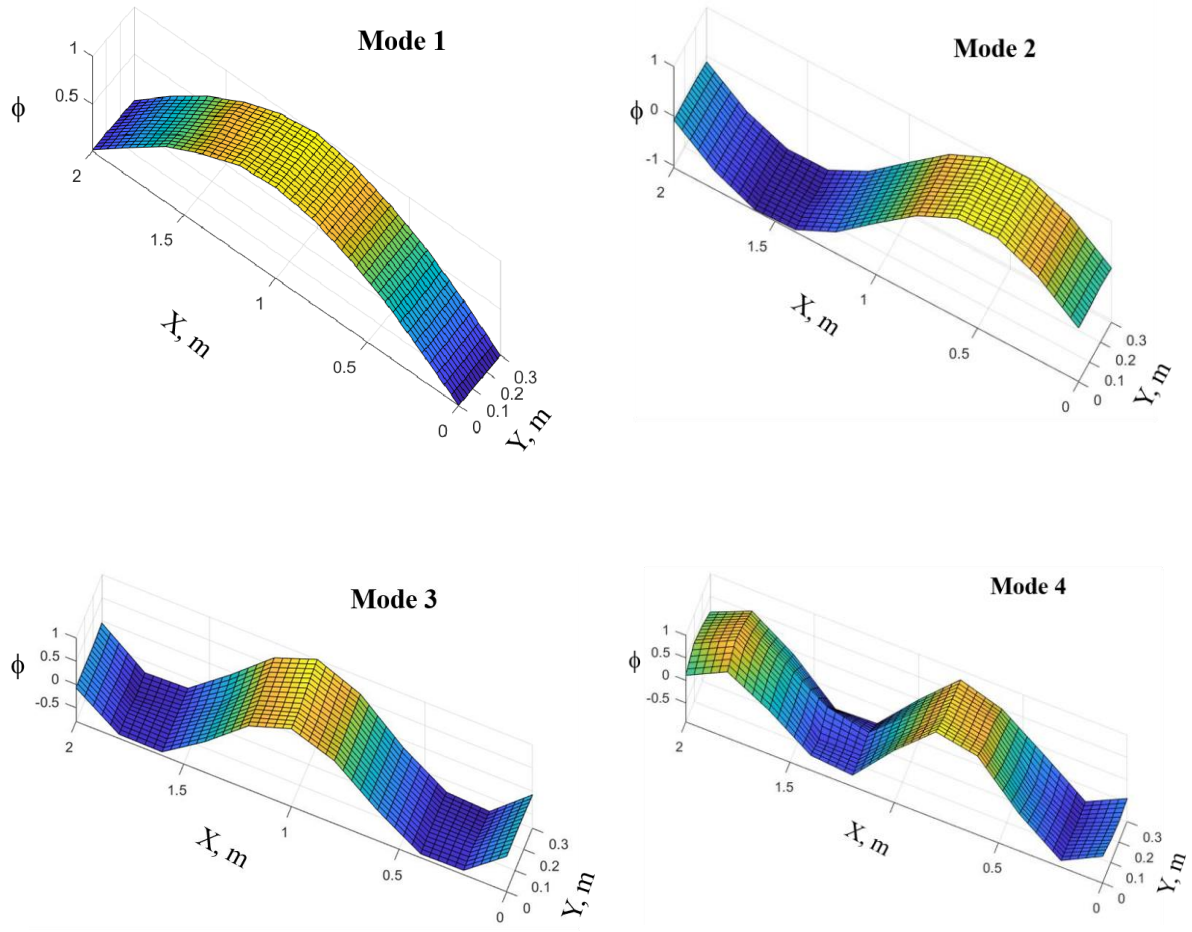

Figure 7. First four bending mode shapes of the steel slab obtained from the experiment

3.2 Finite Element Model

To detect damage using the proposed method, an FE model was created in Sap2000 V22. Figure 8 shows the model in Sap2000. The FE model has the same material properties, boundary conditions and dimensions as the experimental model. The steel modulus elasticity and density are $E_s = 200000$ MPa and $\rho = 7820\ \mathrm{kg/m^3}$, respectively. Shell finite elements are used for simulating slab systems. A Shell is a four-node area object, and each node has six degrees of freedom: three translations and three rotations. 1020 shell elements have been used to model the steel slab. For verification, the Modal Assurance Criterion Analysis (MAC) values of the first four bending mode shapes identified from the FE model and experiment were calculated. Figure 9 shows the MAC matrix. All four modes have a value higher than 0.9, which means that the first four bending mode shapes from FE model and Experiment are identical. Table 1 compares four natural frequencies got from the FE model and experimental testing. The differences between the FE model and experiment are small, less than 4% for each mode. The results proved that the mode shape and frequency of the FE model and experiment are identical. This FE model will be used for further research.

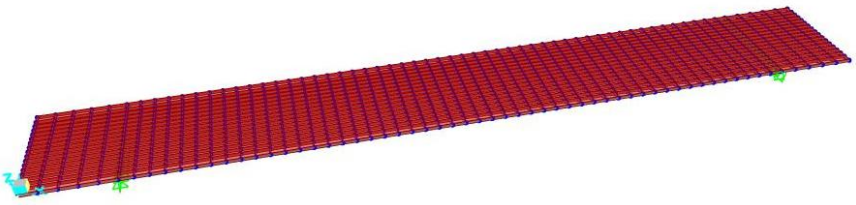

Figure 8. The FE model of the steel plate

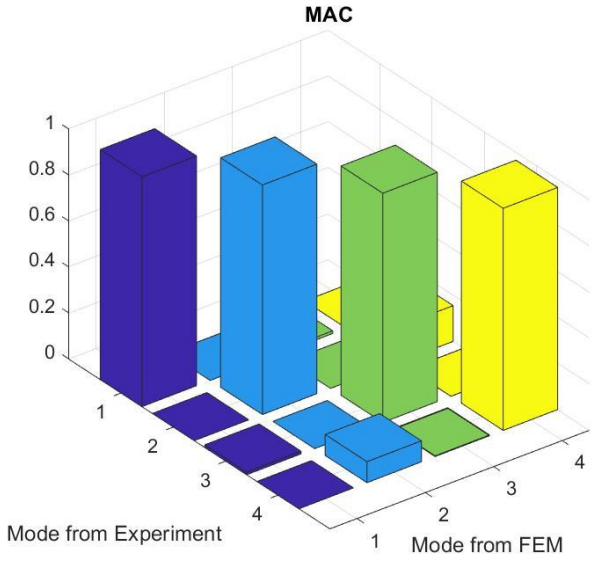

Figure 9. MAC matrix comparing a set of first four bending modes.

Table 1. Natural frequencies (Hz) of the steel plate

Mode Number	1	2	3	4
Experiment	5.74	21.89	45.95	72.35
FEM	5.69	21.94	45.49	69.04
Differences (%)	0.8	0.2	1	4.7

4 Damage detection in a steel slab

4.1 Proposed method

4.1.1 Create input image

In this paper, a novel method using 2D curvature mode shape, CNN, and faster R-CNN is proposed for damage detection in a steel slab. First, mode shapes from damaged scenarios established in the FE model need to be collected. From experiments, only the first four bending mode shapes are identified. Therefore, only these mode shapes are used in the proposed methods. The central finite difference method is applied to calculate the 2D modal curvatures, based on Eq.(1) to Eq. (10). Four modes are used to find the total damage indexes. Figure 10a shows the damage indexes calculated from the mode shape of the scenario that has two damage locations. The location and area of damage are

shown in Figure 10b by the red rectangle. The damage indexes are replotted using a contour plot and shown in Figure 10b. This figure will be used as the input image to train the neural network.

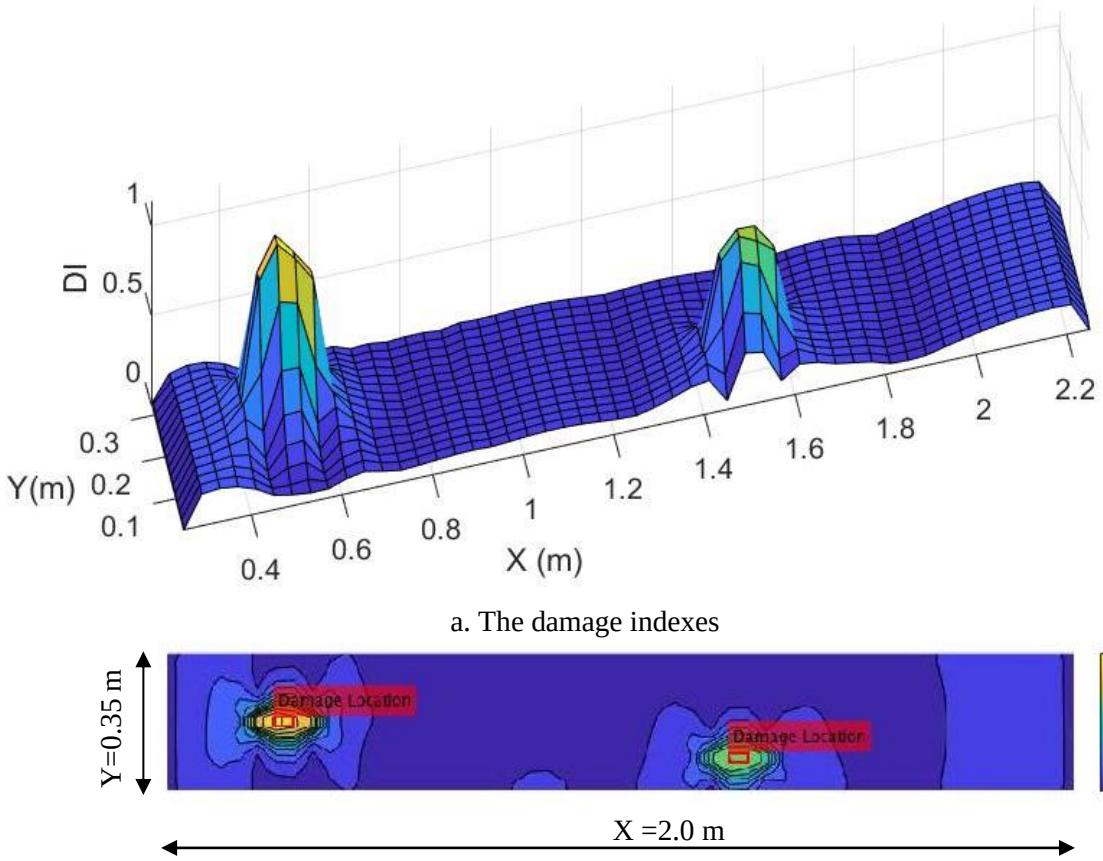

a. The damage indexes

b. Contour Plot (input image)

Figure 10. The damage index and the input image

4.1.2 Identify damage type

Four types of damage with varying levels of severity are considered in this research and shown in Figure 11. The first one (S1) is the single damage, and the second one (S2) is the single damage with a bigger area of damaged hole compared to S1. Multiple damage types are considered as well. M1 and M2 contain two damaged holes. The spacing of the grid line is 0.04m and 0.02m in X and Y directions, respectively. Therefore $(W1, H1) = (0.04, 0.02)$ m and $(W2, H2) = (0.08, 0.04)$ m

A CNN is used to identify damage type based on the damage index calculated using Eq. (1) to Eq. (10). To train the CNN, 400 input images are obtained from 400 damage scenarios. Each damage type has 100 input labelled images. 70% of the dataset is assigned for training and 30% for validation. The image sizes are 104 × 680 pixels. The 5 × 5 kernel is chosen for the CNN calculation. CNN architecture with 16, 32 and 64 filters convolutional layers is used to train and validate the input data set (Figure 12). ReLU (Rectified Linear Unit) is the activation function applied in the convolution layer. Max pooling is applied to decrease the number of parameters. Dropout layers are applied to avoid overfitting. Input Images are classified into four classes S1, S2, M1, and M2 at fully connected layers.

Results obtained after training and validating the proposed CNN are displayed in Figure 13. 25 epochs are used to train CNN. Figure 13 presents the high accuracy of the CNN model for training, more than 90%. The accuracy of the validating data sample is also high, and at some epochs are higher than the training data set, proving no overfitting occurs. Despite the high accuracy, the loss value is

small. The loss value decreases as the number of epochs increases. This means CNN is successfully trained to identify four damage types.

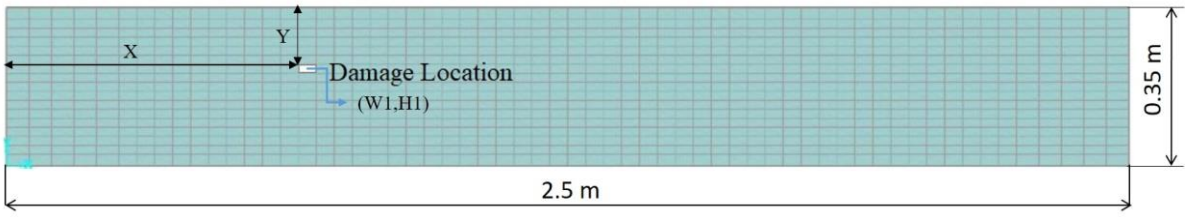

a. S1 damage type

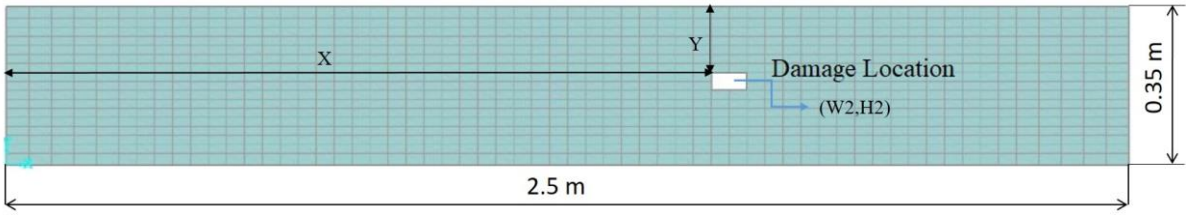

b. S2 damage type

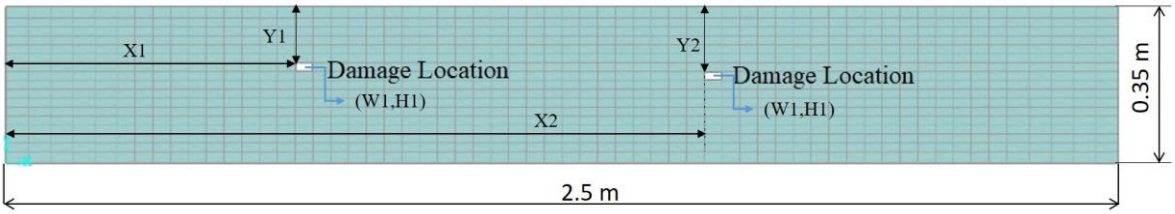

c. M1 damage type

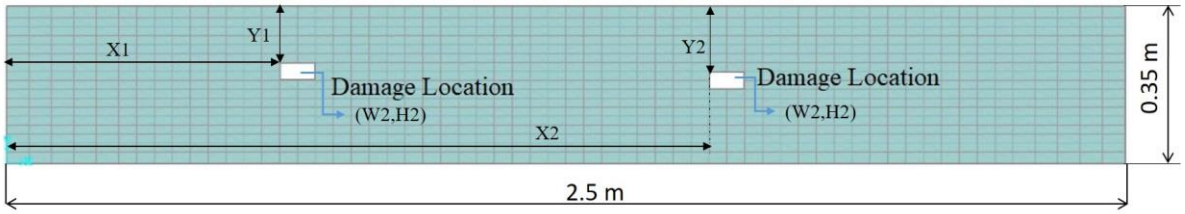

d. M2 damage type

Figure 11. Considered damage types

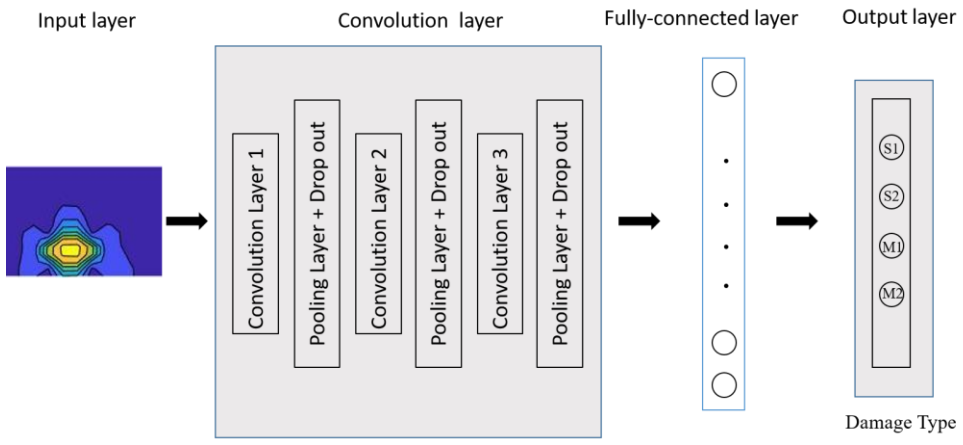

Figure 12. The architecture of a proposed CNN

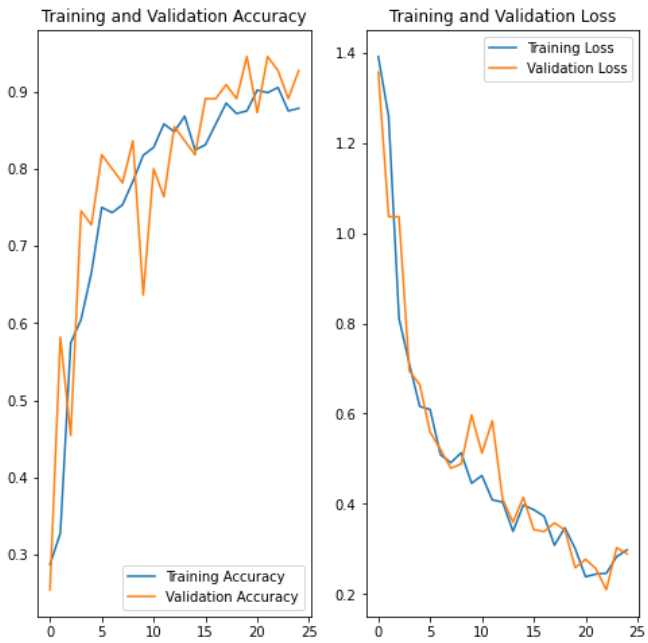

Figure 13. Accuracy and Loss in training and validating CNN model to identify the damage severity type

4.1.3 Identify damage location

For slab structures, one damage location is located along *X* and *Y* direction. One scenario may contain more than one damaged hole. Because the CNN model does not know prior how many damaged holes (objects) are in one picture, it cannot solve this problem. Therefore, faster R-CNN, an object detection model is chosen. Faster R-CNN helps to find every single object in one image. Applying in this paper, faster R-CNN will help to find every single damaged hole from an image obtained from the modal curvature method. As mentioned in section 4.1.2, 400 images from 400 damage scenarios belonging to 4 damage types are created. These images are used again to find the damaged hole. Bounding boxes are used to locate the damage location and to train CNN. One bounding box uses four parameters (X, Y, W1, H1) to describe one damage hole. A scenario which has multiple damage locations is trained with multiple bounding boxes.

After training, the faster R-CNN model can predict the damage location. To improve the accuracy of the model, two damage types are trained separately. S1 and M1 are trained with a neural network. S2 and M2 are trained with another network. The results are shown in Figure 14. After 1000 iterations, the accuracy of the model is nearly 100% for both cases. The loss function value is small and reduced when the iteration increases. However, after 1000 iterations, the accuracy and loss become stable, and the model stops training.

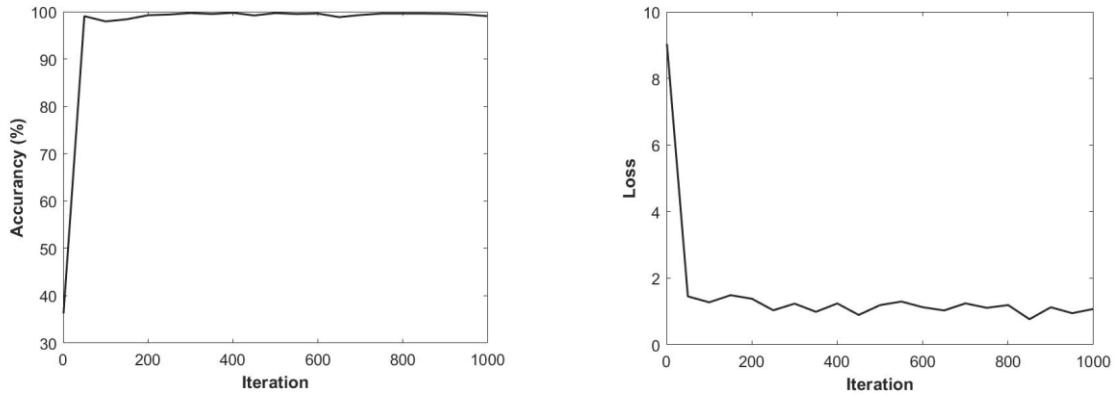

a. S1 and M1 damage type

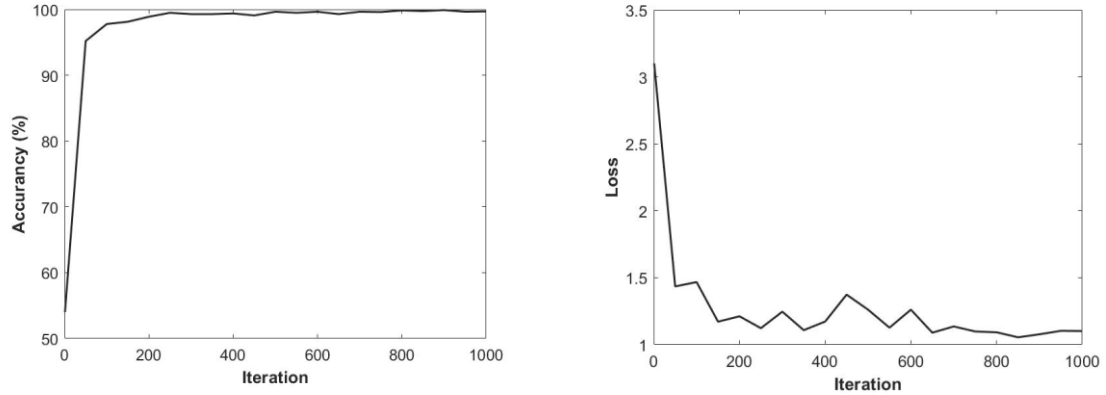

b. S2 and M2 damage type

Figure 14. Accuracy and Loss in training faster R-CNN model to identify damage location

4.2 Verification of the proposed method

4.2.1 Damage scenario examples

To understand the procedure of the proposed method, four damage scenarios presented for S1, S2, M1, and M2 damage types will be presented in detail here. Case 1 with a small single hole (S1 damage type); Case 2 with a bigger single hole (S2 damage type); Case 3 and 4 with two holes (M1 and M2 type). Furthermore, to test the effect of noise on the proposed method, the mode shapes identified from the FE model are polluted with 3% noise. Figure 16 and Figure 17 shows the damage index contour plots calculated from the first four bending mode shape without and with 3% noise, respectively. The damage locations in the slab are presented by the red rectangle. The location and the dimension of the red rectangles are the same as real damages.

The damage type of these eight images will be predicted by the trained CNN. Eight images are used as input of the trained CNN proposed in Section 4.1.2. The predicted results are shown in Figure 15. The trained CNN predicts the damage type of all four damage scenarios with and without noise correctly. The confidence score is the parameter presented for the probability of a scenario belonging to one damage type. Figure 15 shows the high confidence score for all four scenarios. Moreover, when the signal data is polluted with noise, the confidence score shows no significant change. The impact of adding 3% noise on the results of trained CNN is hard to recognize.

These eight images are used as input images of faster R-CNN to find the damage location. The predicted results are presented in Figure 16, and Figure 17 for noise-free, and 3% noise, respectively.

The predicted damage locations are drawn in cyan color. Whereas the real damage locations are drawn in red color. To comment on the accuracy of predicted results, the IoU ratio between predicted and real damage location is calculated. The IoU ratio of all examples scenarios is high. The confidence scores for each box indicating the probability of a damage location are also shown in Figure 16, and Figure 17. Most of those confidence scores are 100%. That means trained faster R-CNN can find out the damaged hole with high confidence and accuracy. Moreover, good results can be found for the added noise cases. Just for Scenario 3, added noise reduces the confidence score and IoU ratio.

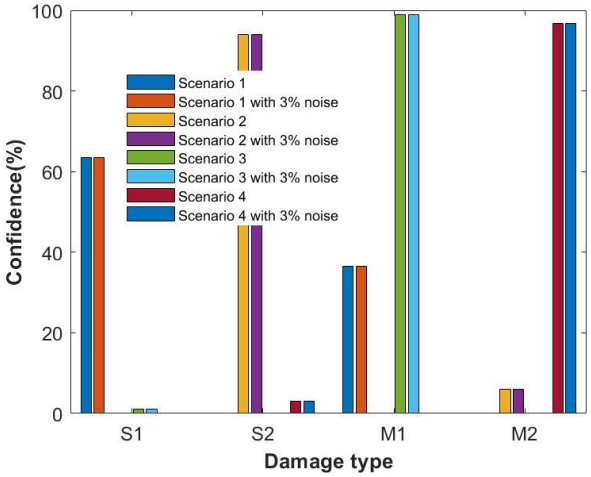

Figure 15. Predicted damage type results for example scenarios

a. Scenario1- S1 damage type; IoU=0.55

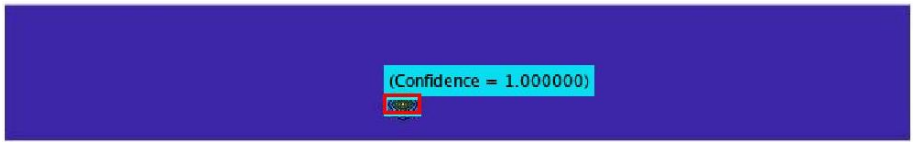

c. Scenario2- S2 damage type; IoU=0.80

c. Scenario3- M1 damage type; IoU=0.77; 0.70

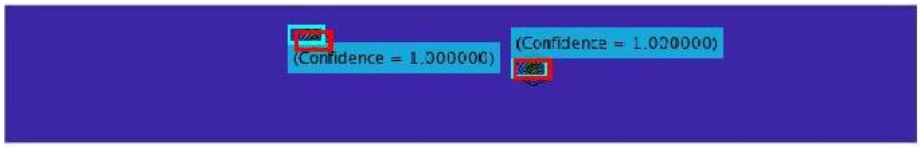

d. Scenario4- M2 damage type; IoU=0.76; 0.79

Figure 16. Damage detection results for example scenario (noise-free). ☐ the real damage location; ☐ the predicted damage location.

a. Scenario1- S1 damage type; IoU=0.55

b. Scenario2- S2 damage type; IoU=0.80

c. Scenario3- M1 damage type; IoU=0.20; 0.57

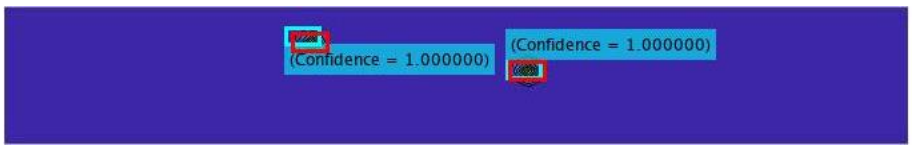

d. Scenario4- M2 damage type; IoU=0.76; 0.79

Figure 17. Damage detection results for example scenario (with 3% noise): ☐ the real damage location and ☐ the predicted damage location.

4.2.2 Test sample set

To evaluate the performance of the proposed method, a test sample set is created. Each damage type S1, S2, M1, and M2 has 60 damage scenarios in this data set. Half of the test set is noise-free, and the other is polluted with 3% noise. Figure 18 shows the confusion matrix of CNN when classifying test damage scenarios into four damage types. Trained CNN classifies 97.5% of scenarios in the test set correctly.

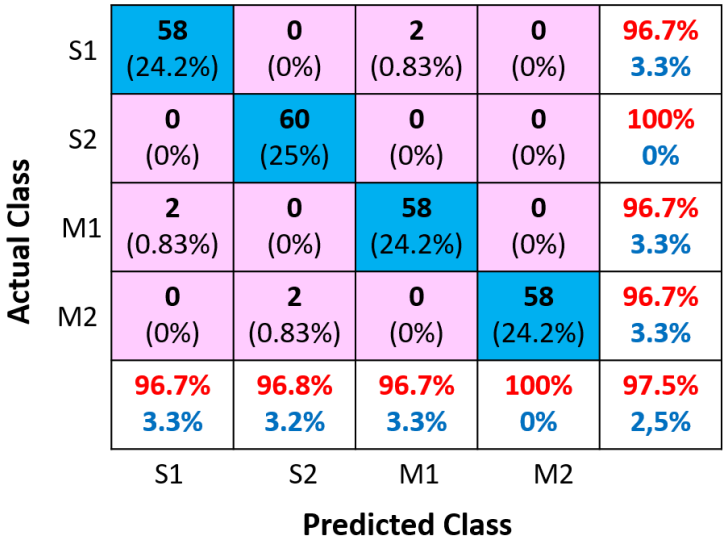

Figure 18. Confusion Matrix for damage type classification

Trained faster R-CNN is applied to find the damage location. For S1 and S2 damage types, from 60 input images, 60 damage locations are found. Whereas M1 and M2 damage types, 120 damage

locations are identified from 60 input images. To evaluate the predicted ability of the model, the Recall to IoU curves is computed and presented in Figure 19. The plots show that for S1, S2 and M2 damage types, 100% scenarios are predicted right with the IoU ratio more than 0.4 %. M1 damage type is an exception. 30% of test scenarios provide the overlap between predicted and real damage location is 0%. The bigger the damaged area, the higher the IoU ratio is recorded.

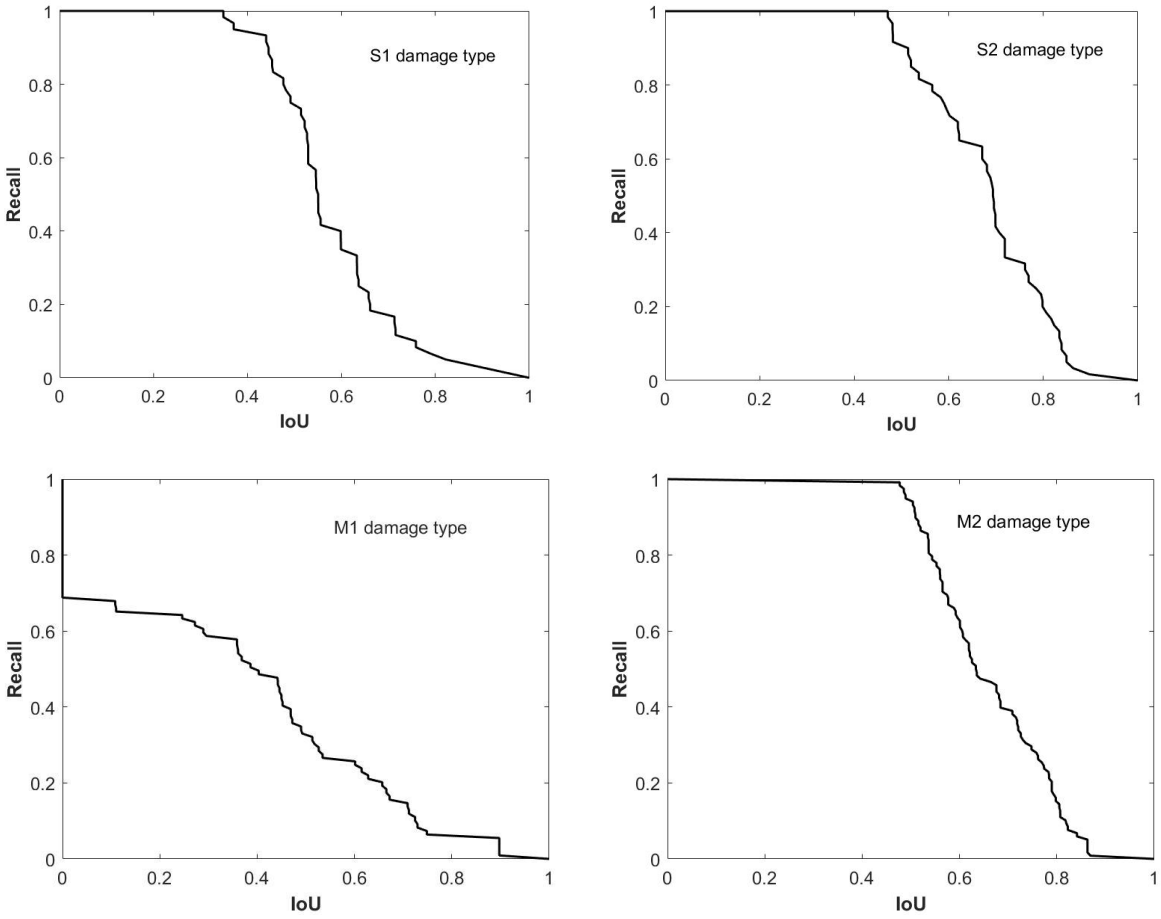

Figure 19. Recall vs IoU overlap ratio on the test sample set

5 Conclusion

This paper uses the 2D modal curvature method to compute damage indexes. The central difference method is chosen to establish the 2D curvature mode shape. Four setups and 16 accelerometers are attached to a simply supported steel slab in a laboratory. Results show that the measured frequencies and mode shapes go well with the numerical ones. The Operational Modal Analysis (OMA) approach and SSI time-domain system identification algorithm help to identify mode shape from measured vibration data fast and reliably.

The drawback of most classical VBDD methods is the difficulty in precisely locating the damage and finding out its severity. In this paper, trained CNN successfully predicts the damage type using images from the 2D curvatures mode shape method as input. Additionally, faster R-CNN can locate the exact location of damage with a high IoU overlap ratio. The test data set with 3% noise added to the mode shapes also shows good results. The test set accuracy of the four damage types classification is 97.5%. For S1, S2 and M2 damage types, the IoU overlap ratio between predicted bounding boxes and the real damage location is more than 0.4. For M1, 30% of scenarios have the IoU ratio equal to 0.

However, M1 is the scenario that has two small damaged holes. Most VBDD methods have difficulty with too small damage severity. These results prove that the proposed method can precisely predict single and multiple damage locations in a slab. Moreover, this method is automatic, easy to perform, and does not need a deep understanding of structural behavior.

In this research, the multiple damage case is the scenario that has two damage locations. It is well known that faster R-CNN can detect several objects in one image. Therefore, more than two locations of damage can be found in one damage scenario in this method. Further research should be done into multiple damage cases. The mode shapes are identified by points in the slabs. Therefore, the prediction accuracy will increase if the network is trained with a tiny mesh size. The architecture of faster R-CNN should be chosen so that high accuracy and no overfitting can be found in the results. Nowadays, measured mode shapes or curvatures can be obtained by using accelerometers [40], wireless sensors [41], and direct modal strain measurements [36]. The number of sensors is not limited. Therefore, the proposed method is robust, effective, and applicable for real structures.

Acknowledgements

This research is funded by the Ministry of Education and Training under grand number B2022-XDA-03.

References

1. Moughty, J.J. and J.R. Casas, *A state of the art review of modal-based damage detection in bridges: Development, challenges, and solutions.* Applied Sciences, 2017. **7**(5): p. 510.
2. Nguyen, H.D., *Monitoring Vietnamese Bridges Using Vibration Based Damage Detection Method and Machine Learning*. 2021, Ghent University.
3. Doebling, S.W., C.R. Farrar, M.B. Prime, and D.W. Shevitz, *Damage identification and health monitoring of structural and mechanical systems from changes in their vibration characteristics: a literature review*. 1996.
4. Fan, W. and P. Qiao, *Vibration-based damage identification methods: a review and comparative study.* Structural health monitoring, 2011. **10**(1): p. 83-111.
5. Pandey, A., M. Biswas, and M. Samman, *Damage detection from changes in curvature mode shapes.* Journal of sound and vibration, 1991. **145**(2): p. 321-332.
6. Ratcliffe, C.P., *Damage detection using a modified Laplacian operator on mode shape data.* Journal of Sound and Vibration, 1997. **204**(3): p. 505-517.
7. Wahab, M.A. and G. De Roeck, *Damage detection in bridges using modal curvatures: application to a real damage scenario.* Journal of Sound and vibration, 1999. **226**(2): p. 217-235.
8. Wu, D. and S. Law, *Damage localization in plate structures from uniform load surface curvature.* Journal of Sound and Vibration, 2004. **276**(1-2): p. 227-244.
9. Qiao, P., K. Lu, W. Lestari, and J. Wang, *Curvature mode shape-based damage detection in composite laminated plates.* Composite Structures, 2007. **80**(3): p. 409-428.
10. Navabian, N., M. Bozorgnasab, R. Taghipour, and O. Yazdanpanah, *Damage identification in plate-like structure using mode shape derivatives.* Archive of Applied Mechanics, 2016. **86**(5): p. 819-830.
11. Zhong, H. and M. Yang, *Damage detection for plate-like structures using generalized curvature mode shape method.* Journal of Civil Structural Health Monitoring, 2016. **6**(1): p. 141-152.
12. Worden, K. and G. Manson, *The application of machine learning to structural health monitoring.* Philosophical Transactions of the Royal Society A: Mathematical, Physical and Engineering Sciences, 2007. **365**(1851): p. 515-537.

13. Azimi, M., A.D. Eslamlou, and G. Pekcan, *Data-driven structural health monitoring and damage detection through deep learning: State-of-the-art review*. Sensors, 2020. **20**(10): p. 2778.
14. Nanthakumar, S., T. Lahmer, X. Zhuang, G. Zi, and T. Rabczuk, *Detection of material interfaces using a regularized level set method in piezoelectric structures.* Inverse Problems in Science and Engineering, 2016. **24**(1): p. 153-176.
15. Samaniego, E., C. Anitescu, S. Goswami, V.M. Nguyen-Thanh, H. Guo, K. Hamdia, X. Zhuang, and T. Rabczuk, *An energy approach to the solution of partial differential equations in computational mechanics via machine learning: Concepts, implementation and applications.* Computer Methods in Applied Mechanics and Engineering, 2020. **362**: p. 112790.
16. Anitescu, C., E. Atroshchenko, N. Alajlan, and T. Rabczuk, *Artificial neural network methods for the solution of second order boundary value problems.* Computers, Materials and Continua, 2019. **59**(1): p. 345-359.
17. Modarres, C., N. Astorga, E.L. Droguett, and V. Meruane, *Convolutional neural networks for automated damage recognition and damage type identification.* Structural Control and Health Monitoring, 2018. **25**(10): p. e2230.
18. Abdeljaber, O., O. Avci, S. Kiranyaz, M. Gabbouj, and D.J. Inman, *Real-time vibration-based structural damage detection using one-dimensional convolutional neural networks.* Journal of Sound and Vibration, 2017. **388**: p. 154-170.
19. Guo, X., L. Chen, and C. Shen, *Hierarchical adaptive deep convolution neural network and its application to bearing fault diagnosis.* Measurement, 2016. **93**: p. 490-502.
20. Cofré, S., P. Kobrich, E.L. Droguett, and V. Meruane. *Transmissibility based structural assessment using deep convolutional neural network*. in *Proc. ISMA*. 2018.
21. De Oliveira, M.A., A.V. Monteiro, and J. Vieira Filho, *A new structural health monitoring strategy based on PZT sensors and convolutional neural network.* Sensors, 2018. **18**(9): p. 2955.
22. Nguyen, T.Q., L.C. Vuong, C.M. Le, N.K. Ngo, and H. Nguyen-Xuan, *A data-driven approach based on wavelet analysis and deep learning for identification of multiple-cracked beam structures under moving load.* Measurement, 2020: p. 107862.
23. Khodabandehlou, H., G. Pekcan, and M.S. Fadali, *Vibration-based structural condition assessment using convolution neural networks.* Structural Control and Health Monitoring, 2019. **26**(2): p. e2308.
24. Nguyen, D.H., T. Bui-Tien, G.D. Roeck, and M.A. Wahab, *Damage detection in structures using modal curvatures gapped smoothing method and deep learning.* Structural Engineering and Mechanics, 2021. **77**(1): p. 47-56.
25. Nguyen, D.H., Q.B. Nguyen, T. Bui-Tien, G. De Roeck, and M.A. Wahab, *Damage detection in girder bridges using modal curvatures gapped smoothing method and Convolutional Neural Network: Application to Bo Nghi bridge.* Theoretical and Applied Fracture Mechanics, 2020. **109**: p. 102728.
26. Saadatmorad, M., R.-A. Jafari-Talookolaei, M.-H. Pashaei, and S. Khatir, *Damage detection on rectangular laminated composite plates using wavelet based convolutional neural network technique.* Composite Structures, 2021. **278**: p. 114656.
27. Ren, S., K. He, R. Girshick, and J. Sun, *Faster r-cnn: Towards real-time object detection with region proposal networks.* Advances in neural information processing systems, 2015. **28**: p. 91-99.
28. Wang, W., B. Wu, S. Yang, and Z. Wang. *Road damage detection and classification with faster r-cnn.* in *2018 IEEE international conference on big data (Big data)*. 2018. IEEE.
29. Cha, Y.J., W. Choi, G. Suh, S. Mahmoudkhani, and O. Büyüköztürk, *Autonomous structural visual inspection using region-based deep learning for detecting multiple damage types.* Computer-Aided Civil and Infrastructure Engineering, 2018. **33**(9): p. 731-747.
30. Wang, B., S. Bai, J. Wang, W. Zhao, Y. Zhang, and Q. Zhang, *A novel concrete crack damage detection method via sparse correlation model.* Structural Control and Health Monitoring: p. e2952.
31. Deng, J., Y. Lu, and V.C.S. Lee, *Concrete crack detection with handwriting script interferences using faster region-based convolutional neural network.* Computer-Aided Civil and Infrastructure Engineering, 2020. **35**(4): p. 373-388.

32. Khatir, S., S. Tiachacht, C. Le Thanh, E. Ghandourah, S. Mirjalili, and M.A. Wahab, *An improved Artificial Neural Network using Arithmetic Optimization Algorithm for damage assessment in FGM composite plates.* Composite Structures, 2021. **273**: p. 114287.
33. Khatir, S. and M.A. Wahab, *A computational approach for crack identification in plate structures using XFEM, XIGA, PSO and Jaya algorithm.* Theoretical and Applied Fracture Mechanics, 2019. **103**: p. 102240.
34. Ho, L.V., T.T. Trinh, G. De Roeck, T. Bui-Tien, L. Nguyen-Ngoc, and M.A. Wahab, *An efficient stochastic-based coupled model for damage identification in plate structures.* Engineering Failure Analysis, 2022. **131**: p. 105866.
35. De Roeck, G., E. Reynders, and D. Anastasopoulos. *Assessment of Small Damage by Direct Modal Strain Measurements*. in *International Conference on Experimental Vibration Analysis for Civil Engineering Structures*. 2017. Springer.
36. Anastasopoulos, D., M. De Smedt, L. Vandewalle, G. De Roeck, and E.P. Reynders, *Damage identification using modal strains identified from operational fiber-optic Bragg grating data.* Structural Health Monitoring, 2018. **17**(6): p. 1441-1459.
37. Girshick, R., J. Donahue, T. Darrell, and J. Malik. *Rich feature hierarchies for accurate object detection and semantic segmentation*. in *Proceedings of the IEEE conference on computer vision and pattern recognition*. 2014.
38. Girshick, R. *Fast r-cnn*. in *Proceedings of the IEEE international conference on computer vision*. 2015.
39. Peeters, B. and G. De Roeck, *Reference-based stochastic subspace identification for output-only modal analysis.* Mechanical systems and signal processing, 1999. **13**(6): p. 855-878.
40. Gordan, M., H.A. Razak, Z. Ismail, K. Ghaedi, Z.X. Tan, and H.H. Ghayeb, *A hybrid ANN-based imperial competitive algorithm methodology for structural damage identification of slab-on-girder bridge using data mining.* Applied Soft Computing, 2020. **88**: p. 106013.
41. Pham, T., E.J. Kim, and M. Moh. *On data aggregation quality and energy efficiency of wireless sensor network protocols-extended summary*. in *First International Conference on Broadband Networks*. 2004. IEEE.